Interpersonal alignment in infra-slow EEG rhythms anticipates mutual recognition

Nicolás Gravel · Tom Froese

Abstract Neuronal rhythms coordinate cognitive and physiological processes across multiple timescales, with slower frequencies potentially forming the basis for meaningful contextual transitions. However, investigating these slower aspects requires methodological innovation beyond standard EEG approaches. Using a minimalist virtual environment paradigm, we found that infra-slow EEG oscillations (ISOs) in the 0.016–0.2 Hz frequency range tracked meaningful contextual transitions during social interaction. Furthermore, participants who successfully engaged in a perceptual crossing task exhibited increased alignment in the spectral power of ISOs when measured in the temporal vicinity of the task response (before-after button press), compared to those who failed. This task-locked alignment was accompanied by similar dynamics in respiratory pressure and electrodermal activity, suggesting that ISOs reflect the integration of physiological, cognitive, and social processes, with their alignment facilitating shared understanding and joint action. These findings highlight the role of ISOs in mediating the temporal dynamics of social cognition and show that inter-participant alignment in ISOs can serve as a proxy for the complex interplay between body physiology, cognition, and social behavior.

Keywords Infra-slow EEG · Haptic stimuli · Interpersonal coordination · Joint action

1 Introduction

Neuronal rhythms occur across multiple spatial and temporal scales, ranging from circuit-level field potentials to system-wide communication between brain and body [1, 2]. Together, they form a complex set of processes that serve as an integrated basis for cognitive and physiological regulation [3]. Across species, these processes are well-aligned with the rhythms of social interaction, including in the case of humans with the fine-grained generation of linguistic utterances as revealed by electroencephalography (EEG) [4, 5]. Semantic content, on the other hand, is highly context sensitive, with narrative integration shown to occur at a time scale of 10 *sec* and more [6]. For example, meta-state transitions in the BOLD signal tend to exhibit a periodicity of around 10 *sec*, and align with salient narrative shifts [7]. This suggests a relationship between slow neuronal and body-wide physiological dynamics [8, 9] and meaningful transitions in social context [10], which should be detectable by other means —including EEG [11].

Here we investigate this relationship within the framework of perceptual crossing [12, 13], a recently established paradigm in social cognition and EEG hyperscanning [14]. This paradigm is designed to facilitate the systematic analysis of real-time social interaction by employing a minimalist approach: It uses binary haptic and auditory feedback to enable intuitive, circular-motion interactions between

Nicolás Gravel
Cognitive Neuroimaging Unit, Institut National de la Santé et de la Recherche Médicale, Commissariat à l'Energie Atomique et aux énergies alternatives, Centre national de la recherche scientifique, Université Paris-Saclay, NeuroSpin, Paris, France
E-mail: nicolas.gravel @ inserm.fr

Tom Froese
Embodied Cognitive Science Unit, Okinawa Institute of Science and Technology Graduate University, Tancha, Onna-son, Okinawa, Japan
E-mail: tom.froese @ oist.jp

two users in a shared virtual environment, allowing them to sense virtual objects and each other's virtual representation through touch or sound. Through this computer-mediated interaction, participants report becoming aware of each other's presence, the onset of which they mark by providing a button press. This enables the assessment of several meaningful transitions, including at the protocol level (rest, pause, task) and task level (before-after button press), which should be detectable in terms of slow EEG rhythms. However, the fast-paced neural rhythms typically recorded with EEG are not a suitable basis for investigating slower aspects of social interaction, which requires methodological innovation. To exploit this potential, here we hypothesize that neuronal and physiological activity at these slow timescales aligns between individuals participating in a social recognition task and that this alignment reflects on infra-slow EEG activity.

To test this hypothesis, we characterized transitions in infra-slow EEG rhythms at the protocol level and at the task level. For the first case, we grouped task trials that were preceded by a resting state period and analyzed all participants, regardless of their performance in the perceptual crossing task. For the second case, the task-level analysis, we defined two groups of participants: one group consisted in pairs that successfully engaged in the perceptual crossing task, recognizing each other presence in the virtual environment, and another group that included pairs that failed to engage. To establish whether distinct dynamic regimes in ISOs in conjunction with physiological activity altered the performance in the task, we tested for inter-participant alignment in the spectral power of ISOs, respiratory pressure and electrodermal activity in the temporal vicinity of the button press.

Our analyses revealed the dynamic nature of ISOs. At the protocol-level, we show a transition from a dominant aperiodic $1/f$ distributed fluctuations and a 0.08–0.12 Hz distributed component during rest, to a gradual increase in a 0.03–0.08 Hz distributed component towards and after task onset, with a subsequent increase in the preponderance of the 0.08–0.12 Hz component during task engagement. Interestingly, at the task-level, both ISOs and physiological measurements (respiration pressure and electrodermal activity) were significantly more aligned between participants who successfully engaged in the task than in those who performed poorly. Moreover, task responses in participants who successfully engaged in the perceptual crossing task were significantly coupled to the phase of the 0.08–0.12 Hz component, with button presses clustering after the crest of the wave. Building on these findings, we propose that ISOs play a pivotal role in mediating the temporal alignment of meaningful transitions between individuals during social interactions, thereby facilitating shared understanding and joint action. As such, inter-participant alignment in ISOs could be taken as a proxy for the emergent, complex interplay between physiology, cognition and social behavior.

2 Results

Our analyses concerned two questions: whether infra-slow EEG rhythms (*e.g.* ISOs) could effectively be shown in the data; and, if they would be able to track meaningful contextual and behavioral transitions. To address these questions, we first characterized the spectral content of the infra-slow EEG data in the 0.016–0.2 Hz frequency range. We then examined the temporal dynamics of two oscillatory distributions within this band, one within the 0.03–0.08 Hz range and another within 0.08–0.12 Hz range (ISOs), focusing on their relationship with task performance.

Figure 1A shows a colored schematic representation of the brain in its bodily context, with visceral organs highlighted in gray. Here we hint at the fact that the brain's rhythms of neural activity are coupled to the body's various physiological rhythms, which may reflect on slower timescales [15] in the EEG (**Fig 1B**). To examine this relationship, we analyzed signals from the brain (electroencephalography, EEG; 0.016–0.2 Hz), the lungs (arbitrary respiration units, ARU; 0.1–0.5 Hz) and the skin (electro-dermal activity, EDA).

Figure 1B shows a representative example of the spectrum (left) and the spectrogram (right) for two participants during a *pre-task* period of 3 minutes including eyes-closed resting state combined with a short eyes-open pause before task onset, and during the subsequent task (1 min). The spectral decomposition of whole-brain infra-slow EEG components revealed the preponderance of two infra-slow oscillations (ISOs), the first with a power distribution peaking within the 0.03–0.08 Hz range, and the second one peaking within the the 0.08–0.12 Hz (see **Supplementary materials**, for details on how we isolated these two ISOs.). These ISOs pointed to dynamic transitions from resting state to task (**Fig S1**). We examined the spatial and temporal aspects of these ISOs in the next analyses.

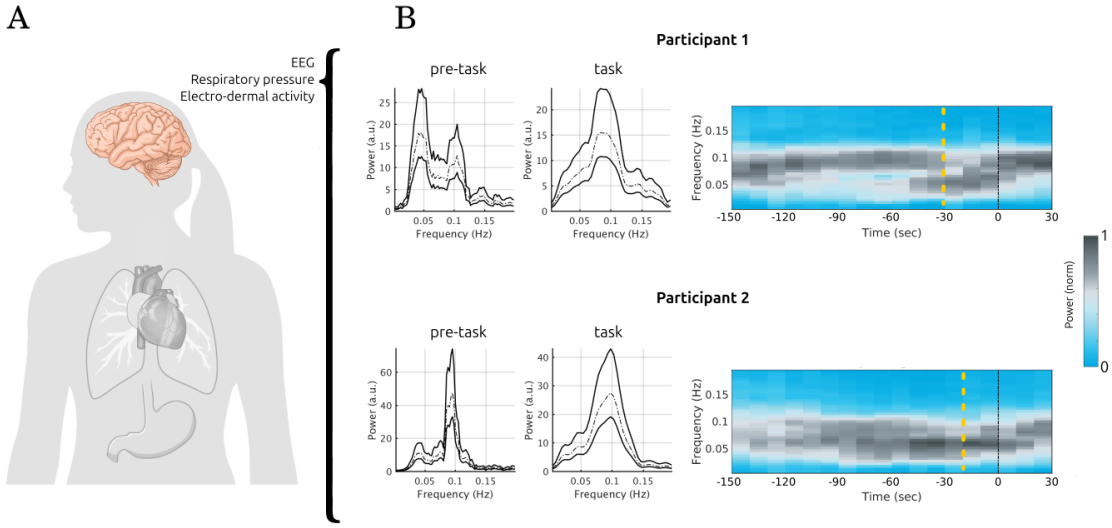

Fig. 1: Brain-body interaction and its footprint in the EEG. (**A**) The brain's rhythms of neural activity are coupled to the body's various physiological rhythms, which unfold on slower timescales. We analyzed signals from the brain (electroencephalography, EEG; 0.016–0.2 Hz), the lungs (arbitrary respiration units, ARU; 0.1–0.5 Hz) and the skin (electro-dermal activity, EDA). (**B**) Representative example of the spectrum ($left$) and the spectrogram ($right$) for two participants during a pre-task trial of 3 minutes including eyes-closed resting state combined with short eyes-open pause before, and during the subsequent task (1 min, eyes-closed). Spectral decomposition of whole-brain infra-slow EEG components revealed the preponderance of two oscillatory peaks, one within the 0.03–0.08 Hz range and another within 0.08–0.12 Hz range. These infra-slow oscillations (ISOs) pointed to dynamic transitions from resting state to task (the vertical dashed yellow line indicate the start of the interim pause period before the task). For methodological details about this figure, see **Supplementary materials**, detailed methods.

2.1 Infra-slow EEG components track behavioral transitions at the protocol level

Figure 2 shows the spectral (**Fig 2A**), temporal (**Fig 2B**) spatial (**Fig 2C**) aspects of the infra-slow EEG power spectra as it unfolds from rest to task. We called this analysis the *protocol-level analysis* because it was conducted on all eligible trials and participants, regardless of their performance in the perceptual crossing task. The goal of this analysis was to reveal the spatio-temporal structure in infra-slow EEG activity, which we did by decomposing spectral activity, averaged for all eligible trials and participants, into non-negative tensor factors (for more details on the tensor factorization approach see **Protocol-level analysis**). This allowed us to summarize the temporal and spatial structure in the spectral power as three distinct frequency factors: a aperiodic $1/f$ distributed factor spanning across all the frequency range of interest (0.016–0.2 Hz); a narrow-band factor with a peak within the 0.03–0.08 Hz range; and a third factor with a broader peak centered within the 0.08–0.12 Hz. The frequency distribution of the second and third factor (**Fig 2A**) closely matched patterns observed in the empirical spectrum (**Fig 1A**), confirming that our factorization captured physiologically meaningful signal components rather than mathematical artifacts. Most importantly, the temporal contribution of these factors (**Fig 2B**) revealed a sequence of transitions that corresponded to different experimental phases: from a broadband $1/f$ distributed pattern, predominant during resting state, to its attenuation towards task onset and the emergence of a dominant period for the 0.03–0.08 Hz distributed pattern towards the end of the resting state period and peaking at task onset, followed by a gradual increase in the prominence of the 0.03–0.08 Hz distributed pattern during active task engagement. A confirmatory analysis included as supplementary material (**Figure S1**) revealed a comparable sequence of transitions. Together, these results confirm that infra-slow EEG rhythms are not only present in the data but exhibit dynamic

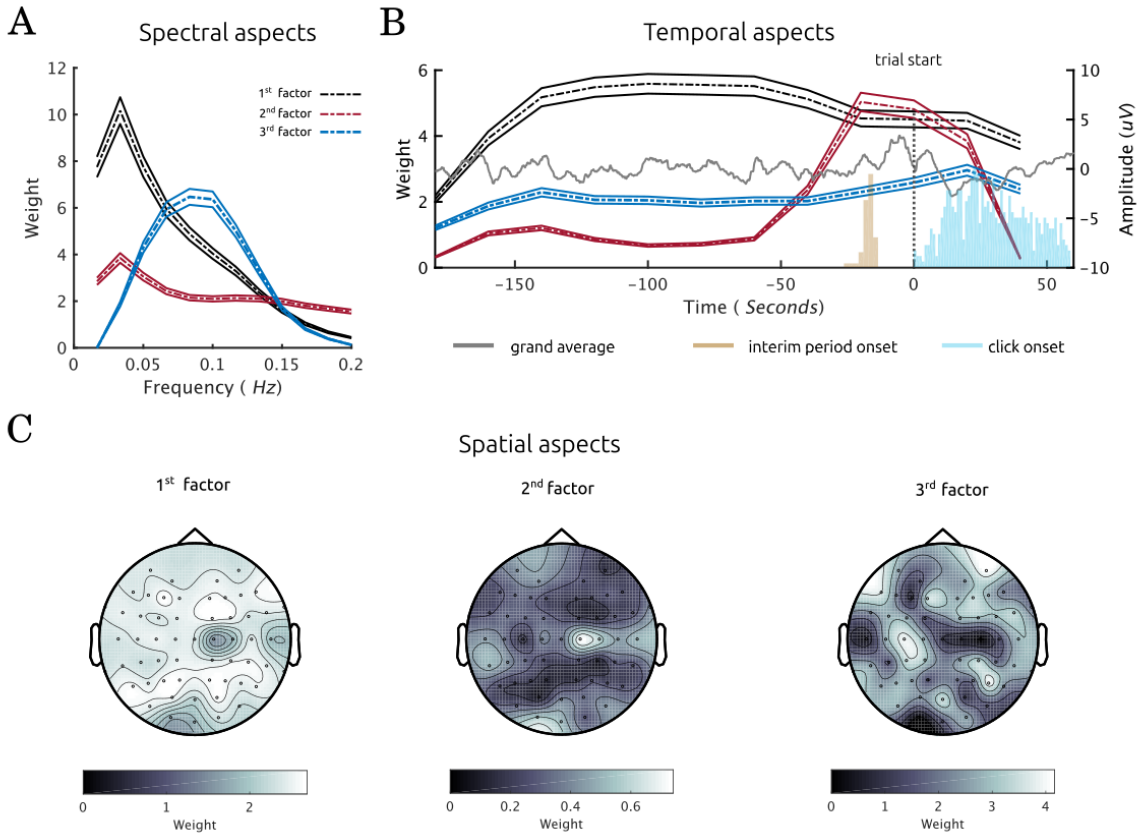

Fig. 2: Factorization of the infra-slow EEG power spectrograms revealed by meaningful transitions at the protocol level. (**A**) To reveal the footprint of ISOs in space and time, we used tensor factorization methods. This resulted in 3 factors with distinct weights for the frequency, temporal and spatial dimension of the tensor. For each dimension, weight magnitudes representing the relative contribution of each factor to the tensor, effectively summarizing the spectral power dynamics unfolding in space and time across the population. As such, the factors thus obtained represent meaningful spaces: $1/f$, the two oscillations identified previously (1), their temporal trajectory (**B**) and their location in the scalp (**C**). The brown and blue histograms are to mark the onset of the interim period and (**B**) the distribution of button presses during the task, respectively. The vertical dotted line indicates the start of the task (see methods section **Protocol-level analysis** for details.).

transitions that align with meaningful contextual changes during resting state and the subsequent task (**Fig 2B**). This transition is further supported by the spatial distribution of these rhythms in the scalp, suggesting that they may play a role in coordinating cognitive and physiological demands during the transition from wakeful rest to social interaction. The spatial aspects revealed a different, complementary picture. Whereas the $1/f$ component showed a more widespread distribution across the scalp, the $<0.05\ Hz$ component was more localized to the occipital and parietal regions (**Fig 2C**), likely reflecting a role for this rhythm in the coordination of visual and motor processing streams before and after task onset, respectively. Concomitantly, the ensuing $0.1\ Hz$ component was characterized by a structured scalp distribution, with several peaks in frontal, lateral and central regions, presumably pointing to long-range correlations between task-positive regions associated with large scale network integration of higher-order cognitive processes involved by the task. We elaborate on this point in the discussion section.

2.2 Inter-participant alignment in infra-slow oscillations anticipates mutual recognition

We then went on to investigate the relationship of infra-slow EEG rhythms with task engagement, and asked whether this relationship was reflected in physiological responses (RP and EDA). To assess these questions, we examined the relationship of task performance with the amplitude and phase of the previous identified ISOs (See **Fig 1B**, **Fig 2** and **Fig S1**), as well as with respiratory pressure (RP) and electrodermal activity (EDA). To achieve this, here we followed a *time-locked* approach and used the linear regression slopes (β) in time-locked activity to summarize the alignment of ISOs and physiological activities between participant pairs in the temporal vicinity of their respective button presses, which participants used to indicate the recognition of each other's presence in the virtual environment. **Figure 3** illustrates the results of this *task-level analysis*. Here the relationship between infra-slow EEG rhythms (as reflected in the two ISOs) and physiological responses to task engagement was assessed by grouping the participants by task performance, defined as the successful or unsuccessful recognition of each other in the haptic virtual space (see *methods* for details on the perceptual crossing experiment). Task responses fell into three categories: joint success (JS), single success (SS), or wrong clicks (W), which we combined into two groups: one group consisted in pairs that successfully engaged in the perceptual crossing task, with both participants recognizing the other's presence (JS); and another group including pairs that failed to recognize the other's presence ($non - JS$). **Figure 3A** shows this relationship through the slope of the linear regression (β) between paired participants' spectral power in ISOs. The higher β in joint success (JS) pairs (dot-dashed lines) compared to unsuccessful ($non - JS$) pairs (dotted lines) indicate similar infra-slow neural dynamics during successful social interaction. This pattern was consistent for both the 0.03–0.08 Hz (red) and 0.08–0.12 Hz (blue) frequency bands. Shuffling button responses to scramble the alignment confirmed the statistical reliability of this finding, with alignment peaks significantly exceeding chance levels (black traces showing 99 %), demonstrating that this similarity in infra-slow neural dynamics was specifically tied to meaningful social interaction rather than coincidental signal fluctuations.

Beyond the alignment in the amplitude of ISOs, we investigated whether ISOs exhibited specific phase relationships to the performance in the task (**Fig 3B**). A Rayleigh test for circular uniformity on the difference between joint success (JS) and $non - JS$ responses (across participants, trials and channels. See **Figure S2** for details.) revealed a distinct significant peak for phase preference past the crest of the wave (between 120–180°) for ISOs in the 0.08–0.12 Hz (Rayleigh test: $p = 0.00064873$, $z = 7.3397$) but not for those in the 0.03–0.08 Hz range (Rayleigh test: $p = 0.055761$, $z = 2.8866$). This frequency-specific phase preference suggests that the 0.08–0.12 Hz rhythm may create temporal windows that optimize social coordination, similar to how faster neural oscillations create optimal windows for perception and action [16]. We elaborate more on this point in the discussion section.

2.3 Greater inter-personal alignment respiratory and dermal activity during joint success

Finally, we examined the alignment of respiratory activity (RP) and electrodermal activity (EDA) (**Fig 3C**). Similarly as with ISOs, we computed the slope of the linear regression (β) between paired participants' physiological signals in the temporal vicinity of task responses. The results showed that respiratory signals were more aligned in JS. This alignment was particularly pronounced right after button click events, indicating that participants' breathing patterns became similar as they recognized each other and completed the task, even though this similarity did not occur simultaneously. Remarkably, EDA signals showed heightened alignment during successful interactions (JS), but decreased alignment during button presses for both JS and $non - JS$ groups, suggesting that autonomic responses become coordinated in anticipation, as well as after, participants responded, regardless of whether they mutually recognized each other's presence in the virtual environment.

Taken together, our findings demonstrate that not only is the alignment in the amplitude of infra-slow oscillations and specific phases at which task-related decisions occur, but also that this alignment extends to physiological processes. This biological meaningful integration of autonomic processes into a shared cognitive and physiological state may show up in participants that successfully recognized each other's presence (JS).

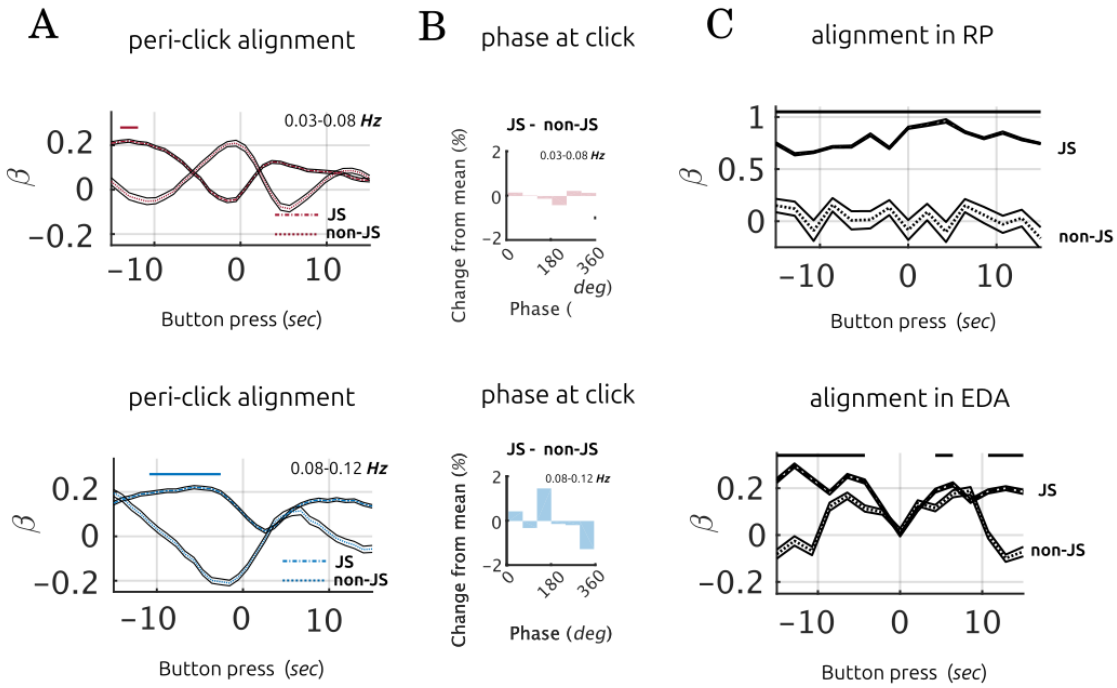

Fig. 3: Inter-participant alignment in task-locked ISO and physiological responses is increased during mutual recognition. (**A**) Inter-participant alignment in the spectral power of ISOs anticipates task success. Colored traces indicate the slope of the linear regression (β) for 1 *sec* epochs (with x–y as participant 1–2) respectively. Black traces indicate the 99 % confidence interval (obtained using 1000 bootstrap iterations with 80 % data resampling to compute the mean and the standard error of the mean). The horizontal colored lines on top of the panels indicate above chance levels for JS computed as the values above null (see methods section **Task-level analysis** for details.). (**B**) Decisions that led to mutual recognition tended to occur past the crest of the 0.08–0.12 Hz wave (between 120–180°). To test for phase preference we computed the differences in percentage change from the mean across channels between JS and $non-JS$ groups. The Rayleigh test for circular uniformity revealed a significant peak for phase preference past the crest of the wave (between 120–180°) for ISOs in the 0.08–0.12 Hz range (Rayleigh test: $p = 0.00064873$, $z = 7.3397$) but not for those in the 0.03–0.08 Hz range (Rayleigh test: $p = 0.055761$, $z = 2.8866$)(See **Figure S2** for details). (**C**) Inter-participant alignment in respiratory (RP) and electrodermal (EDA) du.ring task response. Throughout the peri-click (task-locked) temporal window examined, the respiratory signals display stronger inter-participant coupling in JS (dot-dashed line) compared to $non-JS$ pairs (dotted line). Electrodermal activity, on the other hand, shows a decrease in alignment at the time of button click for both JS and $non-JS$ groups, suggesting that autonomic responses increase their variability as participants click the button, regardless on whether they mutually recognize each other's presence in the virtual environment.

3 Discussion

Neuronal rhythms operate across multiple temporal scales, forming a complex basis for cognitive and physiological regulation. While fast oscillations have been extensively studied for their role in perception and attention, slower rhythms may provide a fundamental scaffold for integrating the brain's various network dynamics [17, 18] with allostatic body processes [9, 15] over the longer timescales necessary for social cognition [6]. Our findings align with this view, demonstrating that infra-slow EEG oscillations orchestrate neural dynamics during social interaction by temporally coupling brain and body activity—a prerequisite for successful joint action. In what follows we discuss the major findings of our study, their

implications for understanding the role of infra-slow oscillations in social cognition, and the methodological considerations involved.

3.1 Methodological considerations

A major challenge in studying infra-slow brain oscillations lies in conventional EEG methodology. Standard recordings typically implement DC-rejection or high-pass filtering at the level of hardware, before digitization, often attenuating or eliminating signals below 0.2 Hz [19]. To overcome this limitation, we employed BrainAmp Standard (brainvision) DC-coupled amplifiers with ultra low cutoff (0.016 Hz). Importantly, we implemented two complementary preprocessing steps to detect lower frequencies. On the one hand we capitalized on high order polynomial removal of aperiodic trends, which we derived from aggressively cleaned data (using strict channel rejection and using the first 8 principal modes for spectral analysis). This complementary step revealed two distinct peaks around <0.05 Hz and 0.1 Hz (**Fig 1B**) that would have been otherwise buried in $1/f$ distributed fluctuations. Although removing non-rhythmic trends that would otherwise dominate the infra-slow frequency spectrum was useful to isolate and visualize the spectral distributions of ISOs, this approach missed the spatial distribution of channels in the scalp (see **Supplementary materials**, detailed methods).

To preserve scalp topology and better interpret our findings, we based our main analyses (with results presented in **Fig 2** and **Fig 3**) on an less stringent approach that included $1/f$ distributed fluctuations and noisy channels (see methods section **Protocol-level analysis** for details.). To this end, we used spherical spline interpolation [20] to remove artifacts without rejecting noisy channels. In this way we could account for the contribution of $1/f$ distributed fluctuations and ISOs to the overall spectral dynamics, while tracking their footprint in time as well as in space. The combination of the two complementary approaches aforementioned enabled us to isolate as well as track the contribution of ISOs effectively in space and time (**Fig 2** and **Fig S1**).

3.2 Possible roles for infra-slow rhythms during social coordination

Our protocol-level analysis revealed a striking sequence of transitions in ISOs that tracked meaningful changes in behavioral state, from rest to task. The sequential transition from a 0.03–0.08 Hz distributed ISO peaking at task onset to an increase in the preponderance of the 0.08–0.12 Hz distributed ISO during task engagement, doubly corroborated in our protocol-level analyses (**Fig 2** and **Fig S1**), suggests that different infra-slow rhythms may reflect distinct functional states: preparation for social interaction and active engagement, respectively [21]. These findings could reflect a number of mechanisms, such as the combined effect of slow readiness potentials during task engagement [22, 16], of the accumulation perceptual evidence [23], and align with emerging evidence that infra-slow fluctuations correspond to different network configurations and cognitive states [18, 17, 24].

One remarkable finding that supports this view is that the <0.05 Hz component was more localized to the occipital and parietal regions (**Fig 2C**). As participants had their eyes open during this interim pause period, we speculate that this spatial pattern may reflect a role for this rhythm in the coordination of visual and motor processing streams at task onset, mirroring our previous findings on the temporal sequences of ISOs. In contrast, the 0.08–0.12 Hz component was localized in frontal, temporal, and parietal areas, known to play a major role in the attentional control of visual processing [25]. Interestingly, given the haptic nature of the task, it is plausible that the interplay of these rhythms may reflect the recruitment of visual and motor areas during haptic exploration. A recent study using fMRI demonstrated a recruitment of foveal retinotopic cortex during haptic exploration of shapes and actions in the dark [26], which lends support to this idea. On the other hand, infra-slow EEG activity is known to be correlated with intrinsic fMRI activity [8, 27], lending extra support to a role of the <0.05 Hz in modulating visual and motor areas.

At the task-level, we linked the results obtained from our data-driven spectral factor decomposition to task performance. To examine inter-participant alignment of brain rhythms, we analyzed the temporal relationship between infra-slow EEG oscillations in participant pairs. In this analysis we move forward from the spectral decomposition approach used previously and use absolute Hilbert envelopes as proxy for spectral power (see methods section **Task-level analysis** for details.). When comparing spectral power

in relationship to task responses (time-locked to button presses), our analysis revealed significantly stronger inter-personal alignment in spectral power for participants who successfully recognized each other compared to those who failed. This alignment was particularly evident in the interval surrounding mutual recognition events (5-10 *sec* before task responses). The alignment observed in the 0.03–0.08 Hz and 0.08–0.12 Hz bands was specifically associated with mutual recognition events and exceeded chance levels derived from jittered response onsets, which scramble the behavioral aspect from the data without changing arbitrary signal properties. This alignment was mirrored by similar patterns in respiratory and electrodermal activity, suggesting enhanced coordination across multiple physiological systems during successful social interaction [28]. Previous research has demonstrated that coupling between infra-slow neural rhythms and autonomic processes occur at different time scales [29, 30]. Illustrative of this, a recent study on joint co-fluctuations of global fMRI activity with physiological signals used cross-correlation to demonstrate two distinct temporal relationships: a negative-to-zero lag peak (-5 to 0 *sec*), suggesting physiological signals follow global fMRI fluctuations, and a positive lag peak (0–10 *sec*), indicating physiological signals may precede fMRI responses [31]. These bidirectional lags may likely point to the integration of top-down cortical modulation with bottom-up peripheral signaling, possibly reflecting system-wide autonomic regulation beyond local vascular effects. Our finding that 0.08–0.12 Hz carried the strongest alignment with task responses, and that this alignment was coupled to the phase of the 0.08–0.12 Hz wave, suggest that such an interplay may well play a role during interpersonal coordination, and that this interplay should be detectable in the EEG signal.

Furthermore, our complementary analysis of phase-task-response coupling revealed that successful mutual recognition events were preferentially clustered past the crest (150–180 *deg*) of the 0.08–0.12 Hz wave. This frequency-specific phase preference suggests that 10–*sec* cycle oscillations may reflect temporal windows that optimize social coordination, similar to how faster neural oscillations create optimal windows for perception and action [16]. Taken together, these findings lend further support to the notion that viscerosensory information modulate perception and cognition through temporal congruency [9], coloring them with value and motivational meaning. According to this view, individuals with greater interoceptive sensitivity may perform better and show enhanced recognition in memory and social tasks [32].

3.3 Broader implications for social cognition and embodied interaction

Our findings have broader implications for understanding the neural basis of social cognition and embodied interaction [33]. Traditional approaches have focused on fast oscillations and event-related potentials, but our results suggest that slower rhythms may as well play an important role in organizing social interactions over extended timescales. Although the precise contribution of visceral and physiological with perception and cognition still remains controversial, the alignment of infra-slow oscillations between individuals may represent previously overlooked mechanism for establishing shared cognitive and physiological states necessary for successful inter-personal coordination [34, 35]. This perspective aligns with theories emphasizing the embodied and interactive nature of social cognition [12, 36], suggesting that the very slow dynamics of neural activity provide a temporal scaffold upon which more rapid cognitive processes unfold.

A recent study using EEG and magnetoencephalography (EMG) to study the dynamics of intentional behavior [37] have suggested that error detection arise from the interplay of two type of signals: a fast unconscious motor code, based on direct sensory and motor pathways, and a slower motor conscious intention that computes the required motor response given the stimulus and task instructions [38]. In accordance with this *dual-route* model of slow conscious versus fast nonconscious evidence accumulation, our finding that correct task responses were coupled to the phase of the 0.08–0.12 Hz extend the notion of this dual-route processing to the infra-slow timescale, suggesting a role for slower visceral nonconscious components in shaping intentional behavior. This role would be to provide a slower nonconscious physiological context for the interplay of slow-conscious and fast-nonconscious codes during the shaping of intentional and social behavior [37, 16].

Slow amplitude modulation of faster oscillations, which has been shown to be a mechanism for the integration of sensory information [16], could also help explain how infra-slow rhythms facilitate the temporal alignment necessary for successful joint action. However, further research is needed to elucidate the precise mechanisms underlying this relationship and how it may vary across different social contexts and modalities. As noted, the brain's amplitude modulation patterns crucial in shaping perception [39]

and action may not be unique to the brain but extend to slower timescale that implicate the internal and external milieus in service of adaptive and efficient social behavior. Our findings support this view that infra-slow rhythms may serve role in social cognition, providing a temporal framework for coordinating complex interactions between individuals.

Future research should investigate whether these patterns generalize to other forms of social interaction and whether they can predict social outcomes in clinical populations with social impairments. Methodological advances enabling the simultaneous measurement of infra-slow brain activity and physiological processes across interacting individuals will be crucial for further understanding the multilevel coordination that characterizes successful social interaction. By elucidating the role of infra-slow EEG rhythms in social cognition, we may prompt new ways of looking into the neural mechanisms underlying shared understanding and joint coordination, with implications for both basic and clinical research in social neuroscience.

4 Methods

4.1 Experimental setup and data characteristics

We utilized an established paradigm known as the haptic perceptual crossing experiment (PCE) [12, 13], which enables systematic investigation of social interaction dynamics. In the PCE paradigm, participants attempt to recognize each other's presence in a minimalist virtual environment through haptic feedback, resulting in one of three possible outcomes: mutual recognition (joint success, JS), one-sided recognition (single success, SS), or no recognition (wrong click, W). Data were collected from 31 experimental sessions, each involving two participants completing eighteen 1-minute trials.

For data analysis, we distinguish two experimental aspects which we call protocol-level and task-level. The protocol-level analysis focused on describing the overall dynamic pattern of infra-slow EEG rhythms during transitions from rest to task states, regardless of task performance. Here we focused on task trials that were preceded by a resting state period (followed by a short pause (or *interim* period) period where one participant had to initiate the task). Concomitantly, to untangle the role of these components during the task, the task-level analysis aimed to elucidate neural and physiological dynamic patterns in the temporal vicinity of task responses. Across all eligible trials for which physiological data were available, we identified experiments in which task responses (time-locked to button press) occurred within 15 *sec* of trial boundaries in both participants. This dual approach allowed us to characterize both the contextual transitions in infra-slow EEG rhythms and the specific patterns associated with successful social interaction.

4.2 Data acquisition and preprocessing

Electro encephalography (EEG) data were acquired using a 64-channel actiCAP system with electrodes positioned according to the standard 10–20 international system. To ensure optimal signal quality, electrode impedances were maintained below 25–35 kΩ through a systematic preparation protocol. The acquisition was conducted using BrainVision Recorder software with a sampling frequency of 1000 Hz. To preserve infra-slow oscillations, we applied a hardware high-pass filter at 0.016-Hz without direct current rejection [21, 27], a critical consideration for capturing slow rhythms frequency range of interest (0.016–0.2 Hz). Additionally, during recording, a 60 Hz notch filter was applied to minimize line noise contamination. We also obtained respiratory pressure (RP) and electrodermal activity (EDA) data from the same participants. See [14] for detailed description of the preparation.

We then down-sampled the EEG data by a factor of 10 (from 1000 Hz to 10 Hz) and removed outlier data using spherical spline interpolation [20], with outliers defined as 10 consecutive points (1 *sec*) exceeding 5 median standard deviation above or below the median computed for a sliding window of 10 *sec*. To recover the spatial footprint of infra-slow EEG rhythms at the protocol level analysis, we spatially whitened the signals obtained in the previous step using generalized eigenvalue decomposition. We used the channel-level covariance data across its total length (rest, pause and task). This step scales the magnitude of the different sensor types relative to one another [40], effectively helping in the recovery of spatial patterns in noisy data with different magnitudes and artifacts across channels. Finally, signals

where demeaned and polynomial trends (order 3) removed from the data. In what follows, we describe the specific analysis steps for both protocol-level and task-level analyses.

A total of 31 experiments were conducted, with each experiment involving two participants. Each participant completed 18 trials, resulting in a total of 558 trials across all experiments. However, only 206 trials contained EDA and RP data. After selecting trials with button presses within the +-15sec from edges range 196 trials were selected for the task-level analysis. For the protocol-level analysis, we selected 62 trials with a resting state period of at least 3 minutes, followed by a short interim period of 10 sec before task onset. This resulted in a total of 124 repetitions.

4.3 Protocol-level analysis

To track meaningful contextual transition at the protocol level, we decomposed the preprocessed EEG data into its spectral components. First, we obtained the power spectral density (PSD) using the multi-taper method [41, 42, 43]. This method provides optimal estimates of spectral concentration by applying multiple orthogonal tapers (Slepian functions) to the signal, reducing variance while maintaining good frequency resolution. We used 7 Slepian tapers with a time-bandwidth product of 4 in the frequency range of 0.016–0.2 Hz resulting in a $[channel \times frequency \times time]$ distribution of spectrograms for each participant and trial. Spectral power was then normalized between 0–1 and averaged across participants and trials to obtain a mean representation of the spectral power dynamics over time. This resulting representation was then used to define non-negative $[channel \times frequency \times time]$ tensor. A complementary approach was used in Figure 1, as explained in supplementary methods.

This tensor was then factorized using canonical polyadic decomposition [44, 45]. This method decomposes the tensor into a sum of rank-one factors. Each factor is the outer product of vectors along different modes of the tensor, enabling the separation of frequency-specific patterns while accounting for their spatial footprint in the scalp (across channels). We implemented a nonlinear least squares algorithm with random factor priors to guide optimization toward an optimal solution [46] and ensure that all components are non-negative and interpretable. We repeated this procedure 10 times to account for random initialization effects, aligning equivalent factors based on their maximum correlation with the first estimation (taken as reference). The mean and standard error of the mean were then reported for the time-frequency factor. This approach allowed us to extract meaningful spectral components from the infra-slow EEG data while preserving their spectral, temporal and spatial structure.

In total, 124 trials were used, with trial-specific spectrograms normalized to 0–1 within experiment and participants. These normalized spectrograms were then averaged across all trials to obtain a mean representation of the spectral power dynamics over time. This resulting representation was then used to define non-the negative $[channel \times frequency \times time]$ tensor. A complementary approach was used in ee **Figure S1**, in supplementary materials.).

4.4 Task-level analysis

To quantify alignment in the spectral power of infra-slow EEG rhythms between participants, we followed a different approach. We first applied a band-pass filter to the preprocessed EEG data in the 0.03–0.08 Hz and 0.08–0.12 Hz frequency ranges using a zero-phase Butterworth filter (order 4). This filtering step was performed to isolate the temporal dynamics of frequency bands of interest that were revealed by out protocol-level analysis, in the temporal vicinity of task responses (± 15 sec around button clicks). We then computed the analytical signal by applying the Hilbert transform on the filtered signals (before epoching to avoiding edge effects from filtering) to obtain, for each channel, the instantaneous phase and amplitude envelope. The absolute magnitude of the amplitude envelope thus obtained was used as a proxy for channel-specific spectral power.

The extent of alignment for each participant pair was quantified using the slope of linear regression between their respective spectral power time series, with higher slope values indicating stronger alignment (with a unity slope representing perfect alignment), zero slope indicating no alignment, and negative slopes indicating anti-alignment. We conducted this analysis on 1 sec epochs. Confidence intervals (CIs) were computed using a bootstrapping approach, where we randomly selected 80 % of the epochs and computed the linear regression slope between paired participants' data. This procedure was repeated

1000 times to generate a null distribution of regression slopes for each task outcome. For this analysis, task outcomes were grouped into a joint success (JS) and non-joint success ($non-JS$) categories. Single success (SS) and wrong (W) responses were grouped into a single "$non-JS$" category as they both represent instances where mutual recognition was not achieved.The 99 percentile of this distribution was used as CIs. To further validate our results, we created a null distribution by randomly jittering the response onset times (100 iterations) and recalculating the regression slopes. This procedure preserved the temporal structure of the signals while disrupting their relationship to behavioral influences unfolding in the temporal vicinity of the button press. Values exceeding the 99 percentile of the null distribution were considered statistically significant alignment patterns that could not be attributed to random fluctuations in the data or general task structure. We also tested random fluctuations in the physiological data data. For respiratory pressure (RP) and electrodermal activity (EDA), we followed a similar procedure to that for infra-slow EEG rhythms, but with longer epochs (2–sec), mean computed from 100 permutations of 50 % random splits, and 30 random shifts on button click onset.

Finally, to examine the phase relationship between task responses and the oscillatory phase of infra-slow EEG rhythms, we constructed phase histograms by binning the instantaneous phase between 0–360 ° using 12 evenly spaced bins. We counted the number of task responses within each bin and converted the counts into percentage signal change from the mean. Since many electrodes were grouped, the resulting distributions were peaking at small changes in the relative frequency, of the order of magnitude of 2–4 percent frequency change. The instantaneous phase was extracted using the Hilbert transform, as described previously. To assess the statistical significance of phase preferences, we applied a Rayleigh test for circular uniformity on the difference between joint success (JS) and $non-JS$ responses. This approach allowed us to specifically test whether successful mutual recognition events had a different phase distribution compared to other task responses.

Across experiments and participants, data from 196 trials were eligible for the task-level analysis. From this pool, 145 trials belonged to the joint success (JS) group, 18 to the single success (SS) group, and 33 to the wrong click (W) group. The $non-JS$ category, which included both SS and W responses, included 51 trials. The number of trials in each group was not balanced, as the task was designed to elicit more successful interactions than unsuccessful ones. This imbalance is a common feature of social interaction tasks, where successful interactions are often more frequent than failures. To assess this unbalance, we used a resampling approach with bootstrapped confidence intervals,a s well as jittered button presses to create a null distribution of regression slopes. This approach allowed us to account for the unbalanced nature of the data while ensuring that the results reflected the natural variability in social interactions.

References

1. Motokawa, K. , Mita, T. , **Das Wahrscheinlichkeitsprinzip über Die Gehirn-Elektrische Erscheinungen Des Menschen**, Japanese Journal of Medical Sciences III (Biophysics) **8**, 63 (1942). Series: Biophysics
2. Singer, W. , **Neuronal Synchrony: A Versatile Code for the Definition of Relations?**, Neuron **24**(1), 49 (1999), doi: 10.1016/S0896-6273(00)80821-1. Doi: 10.1016/S0896-6273(00)80821-1
3. Buzsáki, G. , Draguhn, A. , **Neuronal Oscillations in Cortical Networks**, Science **304**(5679), 1926 (2004), doi: 10.1126/science.1099745
4. Singh, N.C. , Theunissen, F.E. , **Modulation spectra of natural sounds and ethological theories of auditory processing**, The Journal of the Acoustical Society of America **114**(6), 3394 (2003), doi: 10.1121/1.1624067
5. Giraud, A.L. , Poeppel, D. , **Cortical oscillations and speech processing: emerging computational principles and operations**, Nature Neuroscience **15**(4), 511 (2012), doi: 10.1038/nn.3063
6. Varela, F.J. , **Present-time consciousness**, Journal of Consciousness Studies **6**, 111 (1999)
7. Tseng, J. , Poppenk, J. , **Brain meta-state transitions demarcate thoughts across task contexts exposing the mental noise of trait neuroticism**, Nature Communications **11** (2020), doi: 10.1038/s41467-020-17255-9
8. He, B.J. , Raichle, M.E. , **The fMRI signal, slow cortical potential and consciousness**, Trends Cogn. Sci. **13**(7), 302 (2009), doi: 10.1016/j.tics.2009.04.004
9. Critchley, H. , Harrison, N. , **Visceral Influences on Brain and Behavior**, Neuron **77**(4), 624 (2013), doi: 10.1016/j.neuron.2013.02.008
10. Iki, S. , Adachi, I. , **Affective bodily responses in monkeys predict subsequent pessimism, but not vice versa**, Proceedings of the Royal Society B: Biological Sciences **292**(2040), 20242549 (2025), doi: 10.1098/rspb.2024.2549
11. Birbaumer, N. , Elbert, T. , Canavan, A.G.M. , Rockstroh, B. , **Slow potentials of the cerebral cortex and behavior**, Physiol. Rev. **70**(1), 1 (1990), doi: 10.1152/physrev.1990.70.1.1
12. Froese, T. , Iizuka, H. , Ikegami, T. , **Embodied social interaction constitutes social cognition in pairs of humans: A minimalist virtual reality experiment**, Sci. Rep. **4**, 3672 (2014), doi: 10.1038/srep03672
13. Auvray, M. , Lenay, C. , Stewart, J. , **Perceptual interactions in a minimalist virtual environment**, New Ideas in Psychology **27**, 32 (2009)

14. Lerique, S. , Estelle, S. , Hayashi, S. , Leenen, I. , Morrissey, B. , Morrissey, T. , Putri, F. , Uhlig, K. , Zapata-Fonseca, L. , Froese, T. , **The ECSU-PCE Dataset: A comprehensive recording of embodied social interaction with EEG, peripheral physiology, and behavioral measurements in adults**, OSF Preprints (2024), doi: 10.31219/osf.io/6hjfy
15. Engelen, T. , Solcà, M. , Tallon-Baudry, C. , **Interoceptive rhythms in the brain**, Nat. Neurosci. **26**, 1670 (2023), doi: 10.1038/s41593-023-01425-1
16. Schmidt, S. , Jo, H.G. , Wittmann, M. , Hinterberger, T. , **'Catching the waves' − slow cortical potentials as moderator of voluntary action**, Neurosci. Biobehav. Rev. **68**, 639 (2016), doi: 10.1016/j.neubiorev.2016.06.023
17. Gollo, L.L. , Zalesky, A. , Hutchison, R.M. , Heuvel, M. van den , Breakspear, M. , **Dwelling quietly in the rich club: brain network determinants of slow cortical fluctuations**, Philos. Trans. R. Soc. B **369**(1653), 20130521 (2014), doi: 10.1098/rstb.2013.0521
18. Vidaurre, D. , Smith, S.M. , Woolrich, M.W. , **Brain network dynamics are hierarchically organized in time**, Proceedings of the National Academy of Sciences **114**(48), 12827 (2017), doi: 10.1073/pnas.1705120114
19. Kropotov, J.D. , **The enigma of infra-slow fluctuations in the human EEG**, Front. Hum. Neurosci. **16**, 928410 (2022), doi: 10.3389/fnhum.2022.928410
20. Perrin, F. , Pernier, J. , Bertrand, O. , Echallier, J.F. , **Spherical splines for scalp potential and current density mapping**. Short communication EEG02274, U280 Inserm, 151 Cours A. Thomas, 69003 Lyon, France (1989)
21. Monto, S. , Palva, S. , Voipio, J. , Palva, J.M. , **Very slow EEG fluctuations predict the dynamics of stimulus detection and oscillation amplitudes in humans**, J. Neurosci. **28**(33), 8268 (2008), doi: 10.1523/JNEUROSCI.1910-08.2008
22. Deecke, L. , Grözinger, B. , Kornhuber, H.H. , **Voluntary finger movement in man: Cerebral potentials and theory**, Biol. Cybern. **23**, 99 (1976), doi: 10.1007/BF00336013
23. Tsetsos, K. , Pfeffer, T. , Jentgens, P. , Donner, T.H. , **Action Planning and the Timescale of Evidence Accumulation**, PLOS ONE **10**(6), e0129473 (2015), doi: 10.1371/journal.pone.0129473
24. Raut, R.V. , Snyder, A.Z. , Mitra, A. , Yellin, D. , Fujii, N. , Malach, R. , Raichle, M.E. , **Global waves synchronize the brain's functional systems with fluctuating arousal**, Sci. Adv. **7**(30), eabf2709 (2021), doi: 10.1126/sciadv.abf2709
25. Gross, J. , Schmitz, F. , Schnitzler, I. , Kessler, K. , Shapiro, K. , Hommel, B. , Schnitzler, A. , **Modulation of long-range neural synchrony reflects temporal limitations of visual attention in humans**, Proceedings of the National Academy of Sciences **101**(35), 13050 (2004), doi: 10.1073/pnas.0404944101
26. Monaco, S. , Gallivan, J.P. , Figley, T.D. , Singhal, A. , Culham, J.C. , **Recruitment of Foveal Retinotopic Cortex During Haptic Exploration of Shapes and Actions in the Dark**, The Journal of Neuroscience **37**(48), 11572 (2017), doi: 10.1523/JNEUROSCI.2428-16.2017
27. Hiltunen, T. , Kantola, J. , Abou Elseoud, A. , Lepola, P. , Suominen, K. , Starck, T. , Nikkinen, J. , Remes, J. , Tervonen, O. , Palva, S. , Kiviniemi, V. , Palva, J.M. , **Infra-slow EEG fluctuations are correlated with resting-state network dynamics in fMRI**, J. Neurosci. **34**(2), 356 (2014), doi: 10.1523/JNEUROSCI.0276-13.2014
28. Tort, A.B.L. , Laplagne, D.A. , Draguhn, A. , Gonzalez, J. , **Global coordination of brain activity by the breathing cycle**, Nature Reviews Neuroscience **26**(6), 333 (2025), doi: 10.1038/s41583-025-00920-7
29. Kluger, D.S. , Gross, J. , Keitel, C. , **A Dynamic Link between Respiration and Arousal**, The Journal of Neuroscience **44**(47), e1173242024 (2024), doi: 10.1523/JNEUROSCI.1173-24.2024
30. Rebollo, I. , Tallon-Baudry, C. , **The sensory and motor components of the cortical hierarchy are coupled to the rhythm of the stomach during rest**, J. Neurosci. **42**(11), 2205 (2022), doi: 10.1523/JNEUROSCI.1285-21.2021
31. Bolt, T. , Wang, S. , Nomi, J.S. , Setton, R. , Gold, B.P. , deB.Frederick, B. , Yeo, B.T.T. , Chen, J.J. , Picchioni, D. , Duyn, J.H. , Spreng, R.N. , Keilholz, S.D. , Uddin, L.Q. , Chang, C. , **Autonomic physiological coupling of the global fMRI signal**, Nature Neuroscience (2025), doi: 10.1038/s41593-025-01945-y
32. Azzalini, D. , Rebollo, I. , Tallon-Baudry, C. , **Visceral Signals Shape Brain Dynamics and Cognition**, Trends in Cognitive Sciences **23**(6), 488 (2019), doi: 10.1016/j.tics.2019.03.007
33. Lakoff, G. , Johnson, M. , **Philosophy in the Flesh: The Embodied Mind and Its Challenge to Western Thought** (Basic Books, New York, NY, 1999)
34. Bahrami, B. , Olsen, K. , Latham, P.E. , Roepstorff, A. , Rees, G. , Frith, C.D. , **Optimally Interacting Minds**, Science **329**(5995), 1081 (2010), doi: 10.1126/science.1185718
35. Mayer, E.A. , **Gut feelings: the emerging biology of gut–brain communication**, Nature Reviews Neuroscience **12**(8), 453 (2011), doi: 10.1038/nrn3071
36. Jo, H.G. , Wittmann, M. , Borghardt, T.L. , Hinterberger, T. , Schmidt, S. , **First-person approaches in neuroscience of consciousness: Brain dynamics correlate with the intention to act**, Conscious. Cogn. **26**, 105 (2014), doi: 10.1016/j.concog.2014.03.004
37. Charles, L. , King, J.R. , Dehaene, S. , **Decoding the Dynamics of Action, Intention, and Error Detection for Conscious and Subliminal Stimuli**, Journal of Neuroscience **34**(4), 1158 (2014), doi: 10.1523/JNEUROSCI.2465-13.2014
38. Demertzi, A. , Tagliazucchi, E. , Dehaene, S. , Deco, G. , Barttfeld, P. , Raimondo, F. , Martial, C. , Fernández-Espejo, D. , Rohaut, B. , Voss, H.U. , Schiff, N.D. , Owen, A.M. , Laureys, S. , Naccache, L. , Sitt, J.D. , **Human consciousness is supported by dynamic complex patterns of brain signal coordination**, Science Advances **5**(2), eaat7603 (2019), doi: 10.1126/sciadv.aat7603
39. Freeman, W.J. , **A cinematographic hypothesis of cortical dynamics in perception**, International Journal of Psychophysiology **60**(2), 149 (2006), doi: https://doi.org/10.1016/j.ijpsycho.2005.12.009. Models and Theories of Brain Function with Special Emphasis on Cognitive Processing
40. Westner, B.U. , Dalal, S.S. , Gramfort, A. , Litvak, V. , Mosher, J.C. , Oostenveld, R. , Schoffelen, J.M. , **A unified view on beamformers for M/EEG source reconstruction**, NeuroImage **246**, 118789 (2022), doi: https://doi.org/10.1016/j.neuroimage.2021.118789
41. Thomson, D.J. , **Spectrum estimation and harmonic analysis**, Proc. IEEE **70**(9), 1055 (1982), doi: 10.1109/PROC.1982.12433

42. Bokil, H. , Andrews, P. , Kulkarni, J.E. , Mehta, S. , Mitra, P.P. , **Chronux: A platform for analyzing neural signals**, J. Neurosci. Methods **192**(1), 146 (2010), doi: 10.1016/j.jneumeth.2010.06.020
43. Mönke, G. , Schäfer, T. , Parto-Dezfouli, M. , Kajal, D.S. , Fürtinger, S. , Schmiedt, J.T. , Fries, P. , **Systems Neuroscience Computing in Python (SyNCoPy): A Python Package for Large-Scale Analysis of Electrophysiological Data**, Frontiers in Neuroinformatics **18** (2024), doi: 10.3389/fninf.2024.1448161
44. De Lathauwer, L. , De Moor, B. , Vandewalle, J. , **On the best rank-1 and rank-(r_1,r_2,...,r_n) approximation of higher-order tensors**, SIAM Journal on Matrix Analysis and Applications **21**(4), 1324 (2000), doi: 10.1137/S0895479898346995
45. Cichocki, A. , Mandic, D. , De Lathauwer, L. , Zhou, G. , Zhao, Q. , Caiafa, C. , Phan, H.A. , **Tensor decompositions for signal processing applications: from two-way to multiway component analysis**, IEEE Signal Processing Magazine **32**(2), 145 (2015), doi: 10.1109/MSP.2013.2297439
46. Royer, J.P. , Thirion-Moreau, N. , Comon, P. , **Computing the polyadic decomposition of nonnegative third order tensors**, Signal Processing **91**(9), 2159 (2011), doi: 10.1016/j.sigpro.2011.03.006
47. Sadiya, S. , Alhanai, T. , Ghassemi, M.M. , **Artifact Detection and Correction in EEG data: A Review** pp. 495–498 (2021), doi: 10.1109/NER49283.2021.9441341
48. Kantelhardt, J.W. , Koscielny-Bunde, E. , Rego, H.H. , Havlin, S. , Bunde, A. , **Detecting long-range correlations with detrended fluctuation analysis**, Physica A: Statistical Mechanics and its Applications **295**(3–4), 441–454 (2001), doi: 10.1016/s0378-4371(01)00144-3
49. Schafer, R.W. , **What is a Savitzky-Golay filter?**, IEEE Signal Processing Magazine **28**(4), 111 (2011), doi: 10.1109/MSP.2011.941097

Acknowledgments

We are grateful to the Okinawa Institute of Science and Technology Graduate University (OIST) for providing the facilities and support for this research. We would also like to thank Finda Dwi Putri and Chen Lam Loh for their role in EEG signal acquisition and preprocessing and Nicoló Fomento for his help in implementing the spherical spline interpolation for the preprocessing of noisy channels. We also thank the participants for their time and effort in this study.

Funding: N. G. and T. F. were funded by the JST Grant Number JPMJPF2205.

Author contributions: N. G. and T. F. analyzed the data and wrote the manuscript.

Competing interests: There are no competing interests to declare.

Data and materials availability: The data used in this study is available from OSF at `https://osf.io/84wbf/`. The code used to analyze the data is available upon request from the corresponding author and will be made publicly available from GitHub after publication.

5 Supplementary materials

The supplementary materials include the following items:

- **Figure S1**: Factor analysis of spectrograms derived from principal components across grouped trial data.
- **Figure S2**: Phase across channels at button click.
- **Detailed methods**: Complementary preprocessing steps for the isolation of infra-slow EEG oscillations (ISOs) at the protocol level.

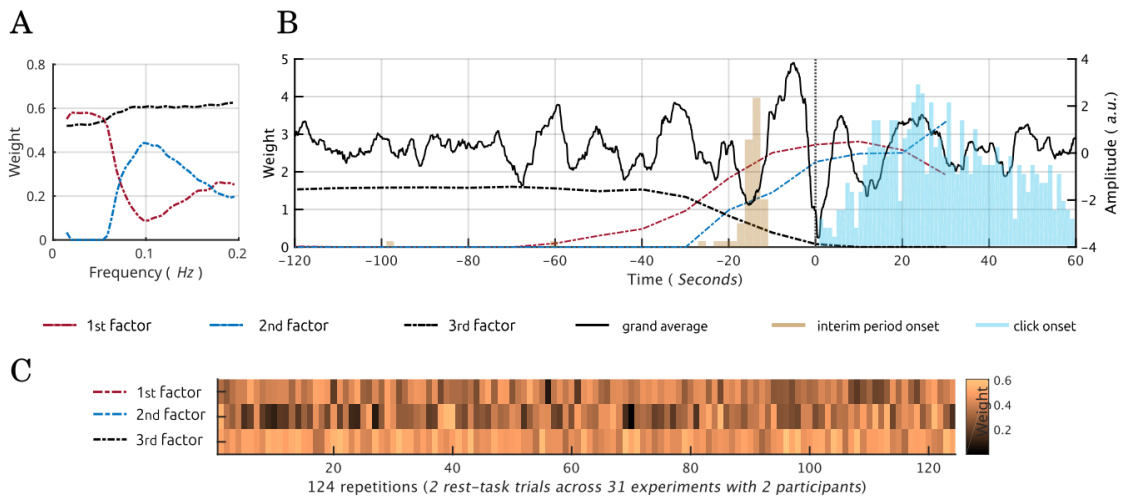

Fig. S1: Temporal evolution and prevalence of infra-slow EEG oscillations across grouped trial data. (**A**) Tensor decomposition of spectrograms (from **Fig 1B**) revealed three factors: a broadband component (dotted black line), a <0.05 Hz peak (dotted red line), and a 0.1 Hz peak (dotted blue line). (**B**) Temporal evolution of factor weights during eyes-closed rest, waiting period, and task. The <0.05 Hz rhythm (red) anticipates rest termination (brown histogram; inset), coinciding with 20 sec EEG amplitude deflections (solid black line). The 0.1 Hz rhythm (blue) aligns with decision-making (blue histogram; button presses). Final 20 sec of task omitted due to spectral edge artifacts. (**C**) Distribution of factor weights across trial repetitions (grouped across experiments and participants). Here the weights indicate the contribution of each trial and participant. This analysis highlighted the presence of infra-slow oscillatory components (ISOs). We extended this analysis to account for aperiodic activity and spatial structure in the main text (**Fig 2C**). Both approaches revealed a similar temporal dynamics, which confirms our approach.

Detailed methods: Isolation of ISOs from aperiodic $1/f$ fluctuations

Several artifact rejection and trend-removal techniques have been proposed, such as higher-order polynomial regression [47, 48]. To isolate ISOs from aperiodic activity and recover their temporal dynamics regardless of channel noise, here we extend on these principles as follows:

- **Downsampling & detrending**: Raw EEG (1000 Hz) was downsampled to 10 Hz. Polynomial trends were subtracted using a sliding-window Savitzky-Golay filter (order=8, window=10 sec) [49], preserving oscillations <0.2 Hz.
- **Channel rejection**: Channels exceeding 3 median absolute deviations (10 sec epochs) were excluded. Retained channels were z-scored within and across channels.
- **Oscillatory mode extraction**: To summarize overall oscillatory patterns in the cleaned data, 8 independent components were derived for time-frequency analysis.

- **Spectral decomposition**: Processed both ICA-derived components (from detrended and normalized data) using the multitaper method [41, 42, 43] using 3 Slepian tapers resulting in one spectrum and spectrogram per trial (including repetitions within experiments).
- **Tensor factorization**: Min-max normalization of the spectrograms across experiments and participants to create a non-negative tensor $[frequency \times time \times trials]$. Applied canonical polyadic decomposition [44, 45], as in main text.

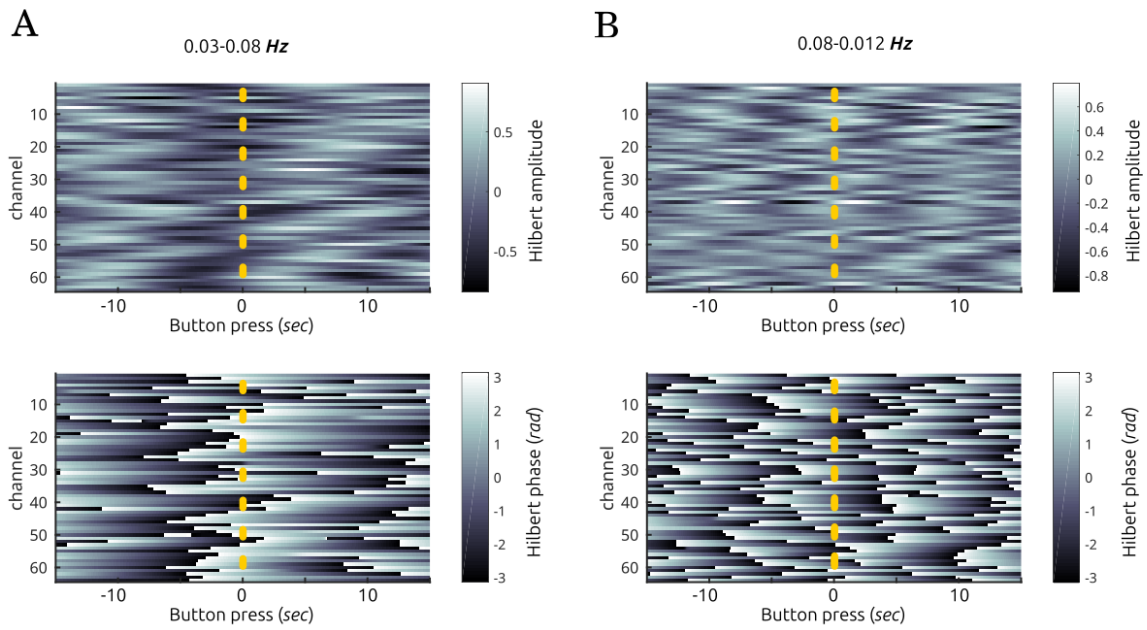

Fig. S2: Amplitude and phase if ISOs across channels. Channel specific amplitude and phase were obtained by computing the real and imaginary parts of the complex analytical signal given by the Hilbert transformation of the preprocessed data (after whitening). This is partly due to the whitening procedure, which emphasize the distributed pattern of ISOs across channels. The amplitude and phase are shown for the 0.03–0.08 Hz (**A**) and 0.08–0.12 Hz (**B**) frequency bands. The absolute value of the amplitude was used to compute alignment in (**Fig 3A**), whereas the phase was used to compute the phase preference in (**Fig 3B**). The vertical yellow dashed line indicate the time of button click. Data for one exemplar participant and trial. Given the wide distribution of phase across channels, we report the percentage signal change from the mean in main text (**Fig 3B**).

We chose this approach for isolate periodic components from aperiodic fluctuations. This helped us visualize the temporal dynamics of ISOs while removing aperiodic $1/f$ distributed fluctuations and noisy channels. The resulting spectrum and spectrograms shown in (**Fig 1B**) illustrated this (for participant 1 and 2, these components explained, respectively, 63.4 % and 68.4 % of the total variation of the preprocessed EEG signals). Note that here we aim to emphasize periodic components and therefore use a slightly different preprocessing pipeline than that used for the analyses in main text (**Fig 2** and **Fig 3**). Briefly, after downsampling we subtracted high order polynomial trends using a sliding window approach. Specifically, a smoothed version of the downsampled signal was computed using a Savitzky-Golay filter [49] (polynomial order = 8, window length = 10 sec), which served as the trend estimate. High order polynomials can approximate slow aperiodic fluctuations, with infinite order approximating periodic oscillations. Based on this trade-off, the chose configuration allowed us to capture slow-varying non-oscillatory components while avoiding the removal of oscillatory activity of interest. The resulting slow-varying non-oscillatory trends were then subtracted from the downsampled signal t. Subsequently, to obtain clean estimates of ISOs, we rejected channels in which the signal was greater than three standard

deviations over the mean for a period of 10 sec at least once during the trial. Eligible channels were then normalized (z-scored across and within channels) and the first 8 main oscillatory modes were extracted using independent component analysis (ICA). We chose 8 ICA components to provide a summary of overall scalp oscillatory patterns. These components were used for time-frequency decomposition and visualization of global patterns. In this way we mitigated the detrimental influence of $1/f$ distributed fluctuations [48] and noisy channels on the detection of ISOs. **Figure 1B** illustrate, for participant 1 and 2, the spectrum and spectrogram obtained from these components (respectively for each participant, they explained 63.4 % and 68.4 % of the total variation of the preprocessed EEG signals). This complementary approach isolated infra-slow oscillations (ISOs) while removing aperiodic $1/f$ distributed infra-slow EEG fluctuations and noisy channels. This helped maintaining spectral-temporal precision at the expense of missing the spatial pattern across channels. Taken together, our dual approach corroborated the presence of infra-slow oscillations (**Fig 1B**) and revealed their temporal dynamics (**Fig 2B** and **Fig S1**), as well as revealed the footprint of ISO components across the scalp (**Fig 1B**). In sum, we provide a heuristic visualization and a rigorous mapping approach to account for the spatial pattern of infra-slow EEG rhythms during social interaction.